JOC The Journal of Organic Chemistry

Note

pubs.acs.org/joc

Aromatic Macrocycle Containing Amine and Imine Groups: Intramolecular Charge-Transfer and Multiple Redox Behavior

Tomohito Ide,[†] Daisuke Takeuchi,[†] Kohtaro Osakada,*[,†] Takashi Sato,[‡] and Masayoshi Higuchi[‡]

[†]Chemical Resources Laboratory, Tokyo Institute of Technology, 4259 Nagatsuda, Midori-ku, Yokohama 226-8503 (Mail Box R1-03), Japan

[‡]Polymer Materials Unit, National Institute for Materials Science (NIMS), 1-1 Namiki, Tsukuba 305-0044, Japan

Supporting Information

ABSTRACT: A cyclic compound that has alternating diphenylamine and quinodiimine units was obtained by condensation of anthraquinone with bis(4-aminophenyl)amine (aniline dimer) in 20% yield. The resulting macrocycle has an absorption of 462 nm, which is assigned to charge transfer transitions between electron-rich diphenylamine units and electron-poor anthraquinone diimine units. Cyclic voltammetry in acidic MeCN shows redox of anthraquinone diimine units ($E_{1/2}$ = 0.03 V vs Ag/Ag^+) and of oxidation of amino groups of higher potentials (0.60 and 0.77 V).

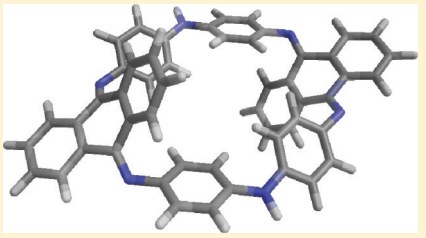

Polyaniline is a typical conductive polymer that shows unique properties such as redox and pH sensitivity.[1] An oxidized form of polyaniline (emeraldine base) contains diaminobenzene and diiminobenzene groups and shows electrical conductivity under acidic conditions. Oligoanilines also hold those properties.[2] Most of the reported oligoanilines have linear structures, and the number of cyclic oligoanilines is limited. A cyclic aniline tetramer was synthesized by Pd-catalyzed coupling of oligoaniline trimer and 1,3-dibromobenzene.[3] Cyclic oligo(*meta*-aniline)s with 4−8 aniline units were prepared by condensation of 1,3-dibromobenzene and 1,3-diamonobenzene catalyzed by Pd complexes.[4]

Recently, Yamamoto reported that $TiCl_4$ promoted the condensation of bis(4-aminophenyl)methane and anthraquinone yielded a macrocycle that consisted of anthraquinone diimine and diphenylene methane groups **AM4** (Scheme 1).[5]

Scheme 1

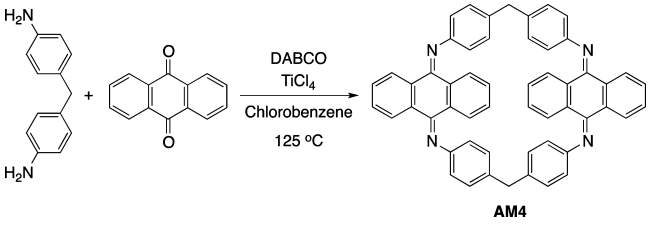

The compound undergoes reversible redox because of the anthraquinone diimine group and accompanying change of color in acidic solution. It prompted us to examine a similar reaction of bis(4-aminophenyl)amine with anthraquinone because it would produce a model compound of the oxidized cyclic oligoaniline.

Herein we report a macrocycle that has alternating diphenylamine and anthraquinone diimine moieties and their properties.

Macrocycle **1** was synthesized according to the preparation procedure of **AM4**;[5] condensation of bis(4-aminophenyl)amine with anthraquinone promoted by $TiCl_4$ produces the desired macrocycle **1** (Chart 1) in 20% yield.

Chart 1

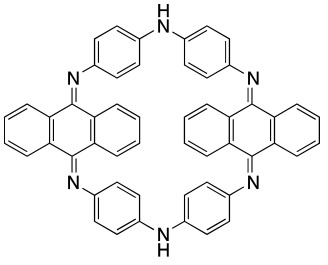

1

The diluted condition (2 mM) and addition of $TiCl_4$ two times during the reaction are important in obtaining **1** in the above yield. Yamamoto already reported the double addition of $TiCl_4$ in the synthesis of **AM4**.[5] The reaction with a higher concentration of the substances and addition of $TiCl_4$ at once resulted in formation of **1** in 1−6%. ^1H NMR spectrum of **1** indicates the cyclic structure with high symmetry. Hydrogens of anthraquinone diimine groups were observed as four double doublet signals. ^{13}C NMR analysis could not be performed because of its low solubility. The high-resolution FAB-MS

Received: August 14, 2011
Published: October 11, 2011

spectrum of **1** shows a signal at m/z = 742.2845, which agrees with calculated exact mass (742.2828).

Vapor diffusion of *n*-hexane into a tetrahydrofuran (THF) solution of **1** gave red crystals. X-ray crystallography revealed the crystal structure including THF and *n*-hexane (Figure 1).

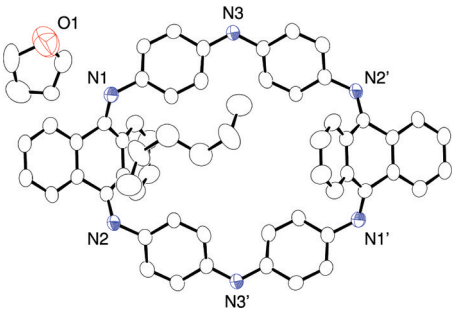

Figure 1. ORTEP drawing of **1**.

The torsion angle between the phenylene groups in diphenylamine unit is 20.7°. It is smaller than that of **AM4** (62.9°),[5] probably because of the delocalization of the lone pairs on the nitrogen atom.

The interaction distance between nitrogen atoms of amino and imino groups is 3.09 Å, which indicates the presence of moderate NH···N hydrogen bonds between the molecules in the crystal. As the result of hydrogen bonds between two imino groups and two amino groups, a two-dimensional hydrogen bond network is constructed as shown in Figure 2a and b.

A UV−vis absorption spectrum of **1** in MeCN contains a broad charge-transfer (CT) absorption band (λ_{max} = 462 nm, 2.68 eV, ε = 1.1 × 10^4 M^{-1} cm^{-1}) corresponding to its red color. To understand the CT transition of **1**, TD-DFT calculation was performed at the PCM-M05-2X[6]/6-31G(2d,p) level using the B3LYP[7]/6-31G(d) geometry by Gaussian 09.[8] The calculated first transition (466 nm, 2.66 eV) mainly consists of a HOMO−LUMO transition with oscillator strength f = 0.00, which suggests that the first transition has an n−π^* nature. The second transition that is main component of the CT band was estimated to be 435 nm (2.85 eV). The main configuration of the second excited state is HOMO-1−LUMO transition with oscillator strength f = 0.52. The HOMO-1 and LUMO of **1** calculated at the B3LYP/6-31G(d) level were illustrated (Figure 3). HOMO-1 is delocalized on diphenylamine units, while LUMO is located on anthraquinone diimine units. Thus, the intramolecular CT transition is rationalized as that occurs between the diphenylamine units (donor) and the anthraquinone diimine units (acceptor).

Cyclic voltammetry of **1** in the presence of trifluoroacetic acid (TFA) showed redox couple at the potential of 0.00 and 0.06 V (vs Ag/Ag^+) caused by anthraquinone diimine component (Figure 4a). Yamamoto assigned the corresponding peak of **AM4** ($E_{1/2}$ = 0.14 V) to one-step redox of four electrons of the molecule in the presence of TFA.[5] In addition, further oxidation of **1** is observed at higher potentials (0.66 and 0.77 V vs Ag/Ag^+). It may be assigned to stepwise oxidation of two amino groups, giving π-conjugated macrocycles without NH hydrogen.

We conducted measurement of the absorption spectra during the electrochemical reduction in the presence of trifluoroacetic acid (TFA) (Figure 4b). Applying the electrochemical potential at −0.10 V (vs Ag^+/Ag) caused disappearance of the CT absorption at 577 nm and increase of the π−π^* transition at ca. 250 nm. It is ascribed to reduction of the anthroquinone diimine into diaminoanthracene. Further applying the potential at +0.30 V recovered the CT transition, indicating reversibility of the electrochemical process.

In summary, we synthesized macrocycle **1**, which has alternating diphenylamine and anthraquinone diimine moieties. The molecule shows the CT transition owing to alternating electron-rich diphenylamine and poor anthraquinone structure. The electrochemical reduction of **1** due to anthraquinone diimine groups occurs at a lower potential than analogous macrocycle **AM4**, and further oxidation of amino groups is also observed.

EXPERIMENTAL SECTION

Synthesis of 1. To a Schlenk tube containing bis(4-aminophenyl)amine (49.8 mg, 0.25 mmol) and anthraquinone (52.1 mg, 0.25 mmol) was added chlorobenzene (80 mL) under argon atmosphere. After the mixture was heated at 125 °C, DABCO (84.6 mg, 0.75 mmol) and chlorobenzene (20 mL) solution of $TiCl_4$ (41 μL, 0.37 mmol) was subsequently added dropwise over 30 min. The mixture was heated at 125 °C for 6 h. The reaction mixture was cooled to room temperature before DABCO (84.1 mg, 0.75 mmol) was added, and then chlorobenzene (20 mL) solution of $TiCl_4$ (41 μL, 0.37 mmol) was added dropwise over 30 min at 125 °C. The reaction mixture was heated at the temperature for 28 h further, cooled to room temperature, and then filtered. The filtrate was evaporated to dryness, and the residue was purified by preparative gel permeation chromatography to afford a bright red solid (18.7 mg, 20%).

Computational Methods. Geometry optimization was performed by B3LYP[7]/6-31G(d) level of theory. Stationary points were characterized by harmonic vibrational frequency analysis. TD-DFT calculation was carried out by M05-2X[6]/6-31G(2d,p) level with

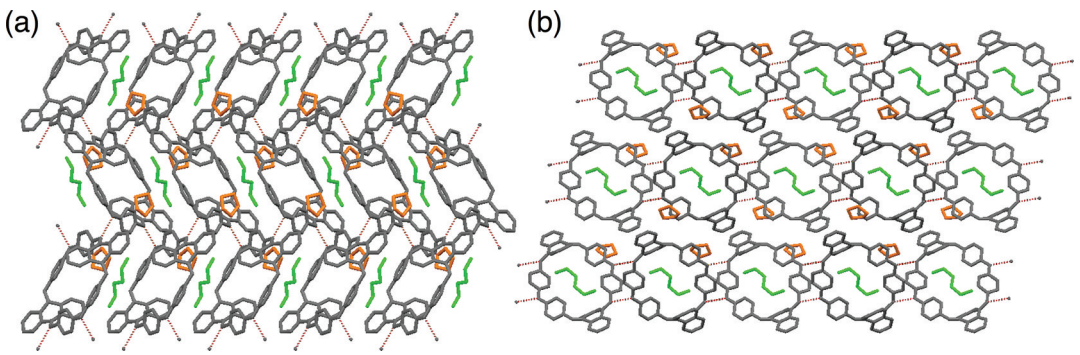

Figure 2. Crystal packing of **1** and hydrogen bonds. (a) View along the *a*-axis; (b) view along the *b*-axis. Red dotted lines show hydrogen bonds.

dx.doi.org/10.1021/jo201650t|J. Org. Chem. 2011, 76, 9504−9506

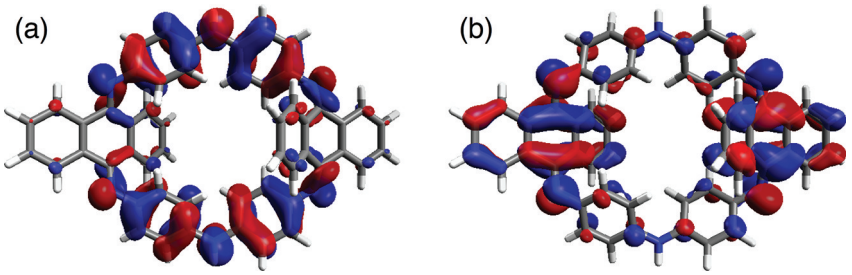

Figure 3. Contour plots of the Kohn–Sham orbitals related to the second excited state: (a) HOMO-1 (−4.81 eV), (b) LUMO (−2.16 eV). Calculated at B3LYP/6-31G(d) level of theory.

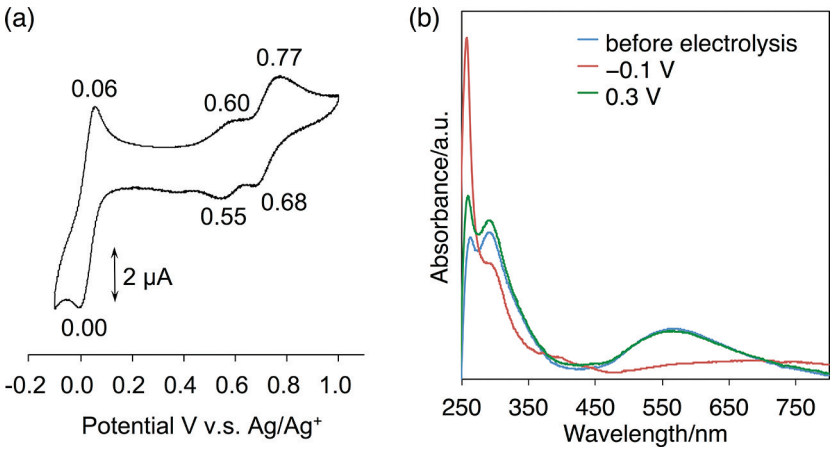

Figure 4. (a) Cyclic voltammogram of **1** (0.20 mM) in MeCN containing 0.10 M nBu$_4$N·PF$_6$ and 0.10 M TFA. (b) Spectroscopic change depending on the applied electrical potential.

IEFPCM (solvent = acetonitrile) solvation model. All calculations were performed by Gaussian 09, B.01.[8] The contour plots (isovalue = 0.02) of the Kohn–Shame orbitals were drawn by Avogadro 1.0.3.[9]

■ ASSOCIATED CONTENT

Ⓢ Supporting Information

NMR and COSY spectra, crystallographic parameters, and computational results of **1** and complete ref 8. This material is available free of charge via the Internet at http://pubs.acs.org.

■ AUTHOR INFORMATION

Corresponding Author

*E-mail: kosakada@res.titech.ac.jp.

■ ACKNOWLEDGMENTS

This work was supported by a Grant-in-Aid for Scientific Research on Innovative Areas, "Coordination Programming" (22108509) from the Ministry of Education, Culture, Sports, Science, and Technology, Japan. T.I. acknowledges a Research Fellowship for Young Scientists from the Japan Society for the Promotion of Science.

■ REFERENCES

(1) (a) Geniès, E. M.; Boyle, A.; Lapkowski, M.; Tsintavis, C. *Synth. Met.* **1990**, *36*, 139–182. (b) Moon, D. K.; Osakada, K.; Maruyama, T.; Yamamoto, T. *Makromol. Chem.* **1992**, *193*, 1723–1728. (c) Kang, E. T.; Neoh, K. G.; Tan, K. L. *Prog. Polym. Sci.* **1998**, *23*, 277–324. (d) Hirao, T.; Higuchi, M.; Ohshiro, Y.; Ikeda, I. *Chem. Lett.* **1993**, 1889–1890. (e) Moon, D.-K.; Ezuka, M.; Maruyama, T.; Osakada, K.; Yamamoto, T. *Macromolecules* **1993**, *26*, 364–369. (f) Moon, D.-K.; Ezuka, M.; Maruyama, T.; Osakada, K.; Yamamoto, T. *Makromol. Chem.* **1993**, *194*, 3149–3155. (g) Higuchi, M.; Imoda, D.; Hirao, T. *Macromolecules* **1996**, *29*, 8277–8279. (h) Gospodinova, N.; Terlemezyan, L. *Prog. Polym. Sci.* **1998**, *23*, 1443–1484. (i) MacDiarmid, A. G. *Angew. Chem., Int. Ed.* **2001**, *40*, 2581–2590. (j) Hirao, T.; Fukuhara, S.; Otomaru, Y.; Moriuchi, T. *Synth. Met.* **2001**, *123*, 373–376.

(2) (a) Sadighi, J. P.; Singer, R. A.; Buchwald, S. L. *J. Am. Chem. Soc.* **1998**, *120*, 4960–4976. (b) Dufour, B.; Rannou, P.; Travers, J. P.; Pron, A.; Zagórska, M.; Korc, G.; Kulszewicz-Bajer, I.; Quillard, S.; Lefrant, S. *Macromolecules* **2002**, *35*, 6112–6120. (c) Gao, J.; Liu, D.-G.; Sansiñena, J.-M.; Wang, H.-L. *Adv. Funct. Mater.* **2004**, *14*, 537–543. (d) Sakurai, H.; Ritonga, M. T. S.; Shibatani, H.; Hirao, T. *J. Org. Chem.* **2005**, *70*, 2754–2762. (e) Wang, Y.; Tran, H. D.; Liao, L.; Duan, X.; Kaner, R. B. *J. Am. Chem. Soc.* **2010**, *132*, 10365–10373. (f) Wei, Z.; Faul, C. F. J. *Macromol. Rapid Commun.* **2008**, *29*, 280–292.

(3) Hauck, S. I.; Lakshmi, K. V.; Hartwig, J. F. *Org. Lett.* **1999**, *1*, 2057–2060.

(4) Fukushima, W.; Kanbara, T.; Yamamoto, T. *Synlett* **2005**, 2931–2934.

(5) Kanazawa, H.; Higuchi, M.; Yamamoto, K. *J. Am. Chem. Soc.* **2005**, *127*, 16404–16405.

(6) Zhao, Y.; Schultz, N. E.; Truhlar, D. G. *J. Chem. Theory Comput.* **2006**, *2*, 364–382.

(7) (a) Becke, A. D. *J. Chem. Phys.* **1993**, *98*, 5648–5652. (b) Stephens, P. J.; Devlin, F. J.; Chablowski, C. F.; Frisch, M. J. *J. Phys. Chem.* **1994**, *98*, 11623–11627. (c) Hertwig, R. H.; Koch, W. *Chem. Phys. Lett.* **1997**, *268*, 345–351.

(8) *Gaussian 09*, Revision B.01; Gaussian, Inc.: Wallingford, CT, 2010. A full reference may be found in the Supporting Information.

(9) *Avogadro: An Open-Source Molecular Builder and Visualization Tool*; Version 1.0.3. http://avogadro.openmolecules.net/.